Decoherence-assisted electron trapping in a quantum dot

Ahmed El Halawany[1,2] and Michael N. Leuenberger[1,2*]
[1] *NanoScience Technology Center, University of Central Florida, Orlando, Florida 32826, USA and*
[2] *Department of Physics, University of Central Florida, Orlando, Florida 32816, USA*

We present a theoretical model for the dynamics of an electron that gets trapped by means of decoherence in the central quantum dot (QD) of a semiconductor nanowire (NW) made of five QDs, between 100 K and 300 K. The electron's dynamics is described by a master equation with a Hamiltonian based on the tight-binding model, taking into account electron-LO phonon interaction (ELOPI). Based on this configuration, the probability to trap an electron with no decoherence is almost 58%. In contrast, the probability to trap an electron with decoherence is 83% at 100 K, 74% at 200 K and 67% at 300 K. Our model provides a novel method of trapping an electron efficienctly at room temperature, which could be used as an electrically driven single photon source (SPS) operating in the wavelength range of $\lambda = 1.3 - 1.5$ μm between 100 K and 300 K.

PACS numbers: 03.67.Bg, 73.23.Hk, 03.65.Yz, 81.07.Ta

Introduction. The interaction between a quantum system and its environment is inevitable, leading to decoherence [1], which is one of the main obstacles in fields such as quantum information processing [2], quantum optics, when measuring optical Schrödinger cat states [3], condensed matter physics, when looking for mesoscopic interference phenomena in quantum transport of electrons [4, 5], etc. Since many interesting quantum phenomena are based on coherence, many solutions are proposed, and are currently in use, to suppress or overcome decoherence [6], such as quantum error-correction codes [7], error-avoiding codes [7], echo techniques [8, 9], quantum feedback operations [3], optimal control technique [10], and many more. Other research groups are trying to fight decoherence through the knowledge of their spectral density, thinking this would be more operative [11]. A rather opposite approach to this stream of research is found in quantum biology, where scientists are trying to take advantage of the decoherence in the quantum dynamics of excitons in order to find explanations for the high efficiency in solar energy harvesting in photosynthetic systems [12, 13]. Recent explanations include environment-assisted energy transfer in quantum networks, such as noise-assisted transport [12, 14] and oscillation-enhanced transport [15, 16].

The idea of an electrically driven SPS, based on Coulomb blockade, was first proposed by Yamamoto's group in 1994 [17]. Since then, many groups have managed to construct such sources [18–21], nevertheless, cryogenic temperatures are essential for the performance of such sources. Such sources, $\lambda = 1.3 - 1.5$ μm, cannot operate above $T = 70$ K. In this letter, we propose a novel physical method that takes advantage of decoherence and results in an enhanced electron trapping probability in the central QD at room temperature. This physical phenomenon can be used as a prototype to build in the future an electrically driven SPS operating at room temperature.

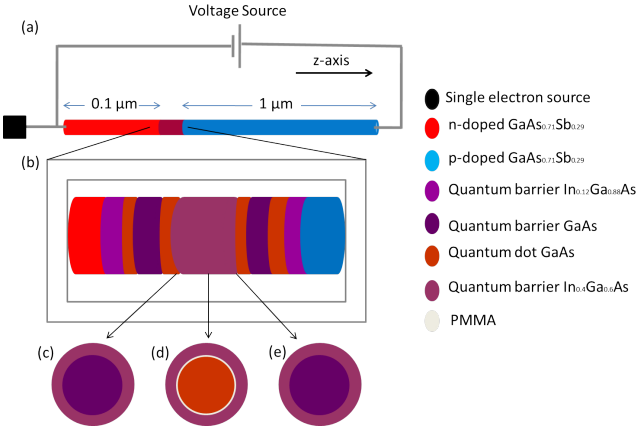

Figure 1: (a) Schematic setup. (b) A magnified diagram for the intrinsic region made of five QDs of (from left to right) 1.8, 1.6, 2.5, 1.6, 1.9 nm height, respectively. (c) A cross section view for the interface between QD #2 and barrier #3. (d) A cross section view for QD #3 (electron pocket). (e) A cross section view for the interface between QD #2 and barrier #4.

Structure and mechanism. We consider the transport of a single electron in a NW with 37 nm in diameter and ~ 1.2 μm in length (see Fig. 1). The NW is divided into three regions. The first (third) region, 0.1 (1) μm in length, is made of $GaAs_{0.71}Sb_{0.29}$ and is n(p)-doped with a concentration of 6.0×10^{14} cm^{-3}. As for the second region, which is embedded between the n-doped and p-doped regions, it is made of five InAs QDs with different heights. However, this is not a typical p-i-n junction because QD #5 is n-doped with 7.5×10^{17} cm^{-3}. All doped regions as well as QD #5 are not degenerate semiconductors. Barrier #1 and #6 are made of $In_{0.12}Ga_{0.88}As$, while all the others are made of GaAs. A monolayer of PMMA, which has radius of 13 nm, is coating the region starting from the interface between QD #2 and barrier #3 to the interface of barrier #4 and QD #4. The outer layer, till the surface of the NW, is made of $In_{0.4}Ga_{0.6}As$.

As a result of this concentric configuration, the central QD acts like an *electron pocket* that traps the electron. The semiconductor interface between the n(p)-doped region and barrier #1 (#6) is recognized as the staggered gap (type II). As for the rest of the interfaces, mainly GaAs/InAs, they belong to the straddling gap (type I). In this work, we use the commonly accepted 60:40 rule for the interfaces. Based on all chosen materials and types of interfaces, the conduction band (CB) profile is shown in Fig. 2. All semiconductor materials have the same crystal structure and direct band gap. The NW is attached to a voltage source in a closed circuit. At the same time, the NW is coupled to a single-electron source (SES) [22, 23]. When the voltage source is off and the configuration is at thermal equilibrium with its environment, the QDs' energy levels are above the chemical potential of the whole configuration. In order to neutralize the built-in voltage and the resulting electric field inside the NW, first, the voltage source is turned on. The voltage is set when the built-in voltage and electric field are neutralized. Only at that point, the electrochemical potential of the QDs fall in the bias windows. Only then the SES is triggered to emit an electron and thus this electron can transport through the whole configuration.

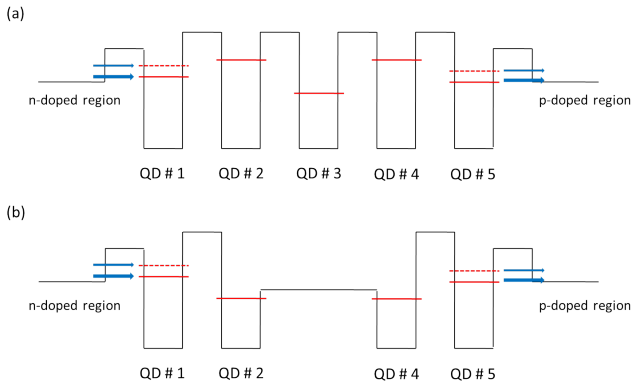

Figure 2: (a) The CB, for radius $R < 13$ nm. (b) The CB, for $R > 13$ nm. The QDs' eigenstates are shown. The solid lines for the ground states $|g, 0\rangle$, while the dotted lines are for the excited states $|e, 0\rangle$. In addition, the sizes of the arrows indicate that the transition rate from the n(p)-doped to the ground states of QD #1 (#5) is 15 times faster than the transition rate to the excited states.

Model. Given that the aforementioned configuration has almost zero electric field across it and electron's eigenenergies are close to the conduction band-edge minima, 3-D time-independent Schrödinger equation, in cylindrical coordinates, using the effective mass approximation is applied for each QD separately. For simplicity, an infinite confining potential in the radial direction is assumed. The eigenenergies and wavefunctions of QDs #1 and #5 are obtained systematically. As for QD #3, due to the relatively large band gap for the

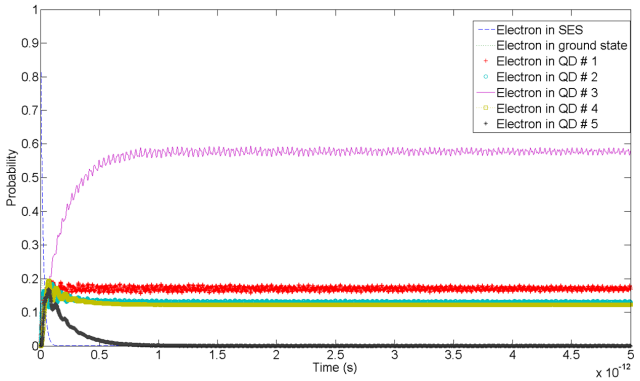

Figure 3: The electron's time-dependent probability distribution among the five QDs in the ZERO-DECOHERENCE case.

PMMA monolayer, it is assumed to be confined in infinite potential but with different radius than QDs #1 and #5. Whereas QDs #2 and #4 require an additional boundary condition due to the electron pocket i.e. the electron's energy has to be conserved irrespective of the interface with GaAs or $In_{0.4}Ga_{0.6}As$ (see Fig. 1). The ground state of this configuration is defined as the state when there is no electron inside the QD heterostructure. The zero energy is set at the minimum of the conduction band of the central QD. For an electron coupled to a heat bath reservoir (phonons), the Hamiltonian is

$$H_0 = \sum_i \varepsilon_i a_i^+ a_i + \left(-\sum_{ij} t_{ij} a_i^+ a_j + \text{h.c} \right) + \hbar\omega_{LO} b^+ b + \lambda \sum_i a_i^+ a_i \left(b^+ + b \right). \quad (1)$$

The first term describes the on-site ground state for the five QDs. The electron's injection to the ground state is 15 times faster than the injection to the excited state. In such systems, where the energy separation is 44 meV, the relaxation takes 20 (40) ps at 300 (100) K [24]. Thus, based on the detailed balance condition, $\frac{W_{nm}}{W_{mn}} = exp\left(-\frac{\hbar\omega_{nm}}{k_B T}\right)$, excitation through phonon assistance will take much longer time. Consequently, excited states can be neglected. The second term, which is based on the tight-binding model, describes the hopping of the electron between the QDs, where t_{ij} is a 3-D hopping integral. In this model, we calculate all ten hopping integrals. Based on the electron-pocket configuration, t_{24} is larger than t_{23} and t_{34}. This is however impossible to achieve in a similar configuration without electron pocket. The third term describes a non-dispersive LO phonon of GaAs. The fourth term describes the interaction between the electron and LO phonons with coupling strength λ. Based on experimental and theoretical works [25, 26], the strength of the ELOPI ($g = \lambda/\hbar\omega_{\text{LO}}$) in QDs, based on their geometry and size, is in the range of 0.5-

1.25. We take $g = 1.0$. However, the final results will not be affected by the value of g. Note that the QDs' ground states will be renormalized, based on the value of g, to $E_g^{'} = E_g - \lambda^2/\hbar\omega_{\mathrm{LO}}$. The validation of the Hamiltonian depends on the following criteria; in this configuration there must be no electrons in the CB. This is calculated in the standard way as follows

$$n = \int_{E_c}^{\infty} D\left(E\right) f^{FD}\left(E\right) dE. \tag{2}$$

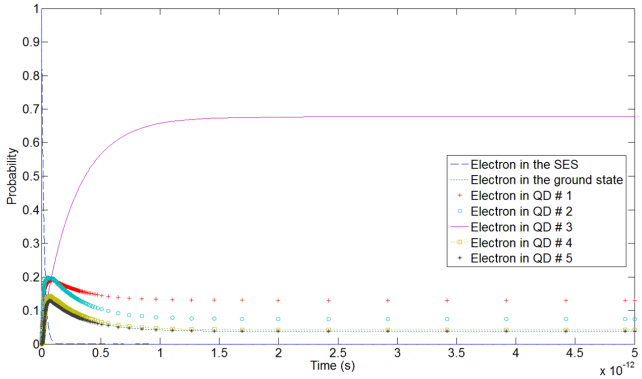

Figure 4: The electron's time-dependent probability distribution among the five QDs at room temperature.

Since the configuration has a large length-to-width ratio, $D\left(E\right)$ is approximated by the density of states of a 1D NW. Doping (type and concentration) along with temperature are taken into account through the Fermi-Dirac function $f^{FD}\left(E\right)$. We observe that irrespective of the electric state of the configuration (on/off), on average there are virtually no electrons in the whole configuration. Consequently, when the SES is triggered and a single electron is emitted, the aforementioned Hamiltonian is a valid description for this single electron. Nevertheless, this Hamiltonian does not describe the coupling between both the n-doped or p-doped regions (quasi-continuum) and QDs #1 and #5, respectively. This coupling is well described by the Fermi's golden rule for transition rates as follows

$$\begin{aligned} W_{i\to f} &= 2\times\frac{2\pi}{\hbar}\sum_i \left|\langle f|H|i\rangle\right|^2 f^{FD}(E_i)\left\{1-f^{FD}(E_f)\right\} \\ &\quad\times\delta\left(E_f - E_i - e\Delta V\right) \end{aligned} \tag{3}$$

where i and f stand for initial and final states respectively. The factor of 2 refers to the spin degeneracy. The hopping integral in Eq. (3) is much smaller than t_{12} and t_{45}. This confirms that we have a weak coupling between the outer QDs and the leads. Thus a standard formalism appropriate for the description of such a system is the generalized master equation in the Born and Markov approximation [27]

$$\partial_t \rho_{m,n} = \frac{i}{\hbar}[\rho, H]_{m,n} + \delta_{m,n}\sum_{l\neq m}\rho_n W_{m,l} - \gamma_{m,n}\rho_{m,n} \tag{4}$$

where $\gamma_{m,n} = \frac{1}{2}\sum_l \left(W_{l,n} + W_{l,m}\right) + \frac{1}{T_2}$ is the total decoherence which includes the dephasing time T_2 due to electron-phonon (both acoustic and optical, and both elastic and inelastic) interaction and the rates $W_{m,l}$ of transition between the leads and the outer QDs. Eq. (4) is valid when the correlation time in the heat bath is much smaller than the relaxation time of the electron system. A rough estimate for the correlation time is $\frac{\hbar}{k_B T} \sim (1-3.5)\times 10^{-14}$ s for T = 100 K - 300 K respectively, which is much smaller than the electron relaxation time, in such systems, $\sim 10^{-12}$ s. The dephasing time T_2, based on temperature, is determined through the homogeneous broadening $2\hbar/T_2$ [28, 29]. At room temperature, the dephasing times are of the order of 200-300 fs [28–30]. We choose $T_2 = 285$ fs at 300 K because there is no carrier-carrier interaction. At T = 100 K, the dephasing time is 2 ps [28–30]. It is worth to mention that we ignore the change in band gap due to the lattice constant mismatch between GaAs and InAs. However, this does not affect the final results. In addition, we disregard any electron-hole interaction until the electron is trapped. For calculating the ground state of QD #5 the doping is taken into account through the Schrödinger-Poisson equation. As a result, the ground state of QD #5 will be $E_g^{'} = E_g - \frac{\lambda^2}{\hbar\omega_{LO}} + \Delta$, where Δ is the increase in the ground energy of QD #5 (few meV) due to doping. The change in wavefunction of QD #5 is negligibly small. Based on this model, there is a ground electron-phonon state with zero phonon $|g, 0\rangle$ in each QD.

Results and discussion. In the numerical calculations using Eq. (4) the trace of the density matrix is equal to one for all times. This assures that the particle conservation principle is not broken. Moreover, it implies that the Hamiltonian is hermitian. In Fig. 3, at $t = 0$, $\rho_{gg} = 1$, hence there is no electron in the configuration. In addition, when there is no decoherence, the probability of the electron to get trapped in the central QD is 58%. On the other hand, when decoherence comes into action, the electron's trapping probability does increase to 67% - 83% depending on the temperature (see Fig. 3 and 4). The probability of the electron's trapping at different temperatures and their corresponding dephasing times are shown in Table I.

Temperature [K]	Dephasing time T_2 [21]	Electron trap [%]
100	2 ps	83
150	667 fs	77
200	500 fs	74
250	334 fs	70
300	285 fs	67

Table I: Probability of electron being trapped in the central QD at various temperatures between 100 K and 300 K.

Although as the dephasing rate increases the trap-

ping probability decreases, it is larger than the "ZERO-DECOHERENCE" case. Many factors contributed to this counter-intuitive result. First, the p-doped region has to be connected through a battery to the n-doped (see Fig. 1). Otherwise, this will be a regular NW and the electron will keep hopping from the n-doped to the p-doped without any chance of getting trapped in any of the QDs. Second factor is the electron pocket, which is essential for the electron to get accumulated in the central QD. Another crucial factor is the fast electron injection from the n-doped region to QD #1 and from QD #5 to the p-doped region. The electron's transition rate (Eq. (3)) from the n-doped to the first QD's ground state $W_{n\to 1g}$ has to be almost 100 times larger than $W_{1g\to n}$. $W_{n\to 1g}$ is $1.5 \times 10^{14}\ s^{-1}$ as well as $W_{5g\to p}$. This fast injection is achieved through two factors: the density of states of the NW and the n-doping of the outer lead. The electron's transition rate $W_{5g\to p}$ has to be almost 100 times larger than $W_{p\to 5g}$. Another contributing factor is the QDs' eigenenergies relative to each other, i.e. if any of the QD's energy level is modified, without adjusting the other QDs' eigenenergies, the trapping efficiency will decrease. Furthermore, the central QD's eigenenergy is the lowest among all QDs. Based on the geometry and the dimensions of the QDs, the energy difference between the central QD's eigenenergy and the neighbor QDs' eigenenergies is almost 110 meV. This means the trapped electron needs to absorb three LO phonons in addition to LA phonon to be able to escape. Even with a strong ELOPI, this process takes more than 1 ns. Thus, our scheme provides an efficient trapping mechanism.

Conclusion. We propose a realistic configuration to trap an electron at high temperature (100 K - 300 K) using decoherence in an electron-pocket configuration. The trapping is achieved in less than 2 ps with a probability ρ_{33} depending on the temperature. At $T = 100$ K, 200 K, 300 K the trapping probability is $\rho_{33} = 83\%$, $\rho_{33} = 74\%$, $\rho_{33} = 67\%$, respectively. Our model can be used to implement an efficient electrically driven single photon source operating at wavelengths $\lambda = 1.3 - 1.5\ \mu$m and between 100 K and 300 K.

We acknowledge support from NSF (Grant No. ECCS-0725514), DARPA/MTO (Grant No. HR0011-08-1-0059), NSF (Grant No. ECCS-0901784), AFOSR (Grant No. FA9550-09-1-0450), and NSF (Grant No. ECCS-1128597). We thank Winston Schoenfeld and Volodymyr Turkowski for useful discussions.

* Electronic address: Michael.Leuenberger@ucf.edu

[1] H.-P. Breuer and F. Petruccione, *The Theory of Open Quantum Systems* (Oxford University Press, New York, 2002).
[2] J. Fischer and D. Loss, Science **324**, 1277 (2009).
[3] S. Deleglise, I. Dotsenko, C. Sayrin, J. Bernu, M. Brune, J.-M. Raimond, and S. Haroche, Nature **455**, 510 (2008).
[4] A. van Oudenaarden, M. Devoret, Y. Nazarov, and J. Mooij, Nature **391**, 768 (1998).
[5] A. Bachtold, C. Strunk, J. Salvetat, J. Bonard, L. Forro, T. Nussbaumer, and C. Schonenberger, Nature **397**, 673 (1999).
[6] J. R. Anglin, J. P. Paz, and W. H. Zurek, Phys. Rev. A **55**, 4041 (1997).
[7] P. W. Shor, Phys. Rev. A **52**, R2493 (1995).
[8] H. Bluhm, S. Foletti, I. Neder, M. Rudner, D. Mahalu, V. Umansky, and A. Yacoby, Nat. Phys. **7**, 109 (2011).
[9] J. Petta, A. Johnson, J. Taylor, E. Laird, A. Yacoby, M. Lukin, C. Marcus, M. Hanson, and A. Gossard, Science **309**, 2180 (2005).
[10] H. Rabitz, R. de Vivie-Riedle, M. Motzkus, and K. Kompa, Science **288**, 824 (2000).
[11] G. A. Álvarez and D. Suter, Phys. Rev. Lett. **107**, 230501 (2011).
[12] M. Mohseni, P. Rebentrost, S. Lloyd, and A. Aspuru-Guzik, J. Chem. Phys. **129** (2008).
[13] F. Caruso, A. W. Chin, A. Datta, S. F. Huelga, and M. B. Plenio, J. Chem. Phys. **131** (2009).
[14] M. B. Plenio and S. F. Huelga, New J. Phys. **10** (2008).
[15] F. L. Semiao, K. Furuya, and G. J. Milburn, New J. Phys. **12** (2010).
[16] S. Lloyd and M. Mohseni, New J. Phys. **12** (2010).
[17] A. Imamoglu and Y. Yamamoto, Phys. Rev. Lett. **72**, 210 (1994).
[18] P. Michler, A. Kiraz, C. Becher, W. Schoenfeld, P. Petroff, L. Zhang, E. Hu, and A. Imamoglu, Science **290**, 2282+ (2000).
[19] C. L. Salter, R. M. Stevenson, I. Farrer, C. A. Nicoll, D. A. Ritchie, and A. J. Shields, Nature **465**, 594 (2010).
[20] S. Kako, C. Santori, K. Hoshino, S. Goetzinger, Y. Yamamoto, and Y. Arakawa, Nat. Mater. **5**, 887 (2006).
[21] S. Strauf, N. G. Stoltz, M. T. Rakher, L. A. Coldren, P. M. Petroff, and D. Bouwmeester, Nat. Photonics **1**, 704 (2007).
[22] G. Feve, A. Mahe, J. M. Berroir, T. Kontos, B. Placais, D. C. Glattli, A. Cavanna, B. Etienne, and Y. Jin, Science **316**, 1169 (2007).
[23] E. Bocquillon, F. D. Parmentier, C. Grenier, J.-M. Berroir, P. Degiovanni, D. C. Glattli, B. Placcais, A. Cavanna, Y. Jin, and G. Fève, Phys. Rev. Lett. **108**, 196803 (2012).
[24] S. Sauvage, P. Boucaud, R. Lobo, F. Bras, G. Fishman, R. Prazeres, F. Glotin, J. Ortega, and J. Gerard, Phys. Rev. Lett. **88** (2002).
[25] R. Heitz, I. Mukhametzhanov, O. Stier, A. Madhukar, and D. Bimberg, Phys. Rev. Lett. **83**, 4654 (1999).
[26] M. A. Odnoblyudov, I. N. Yassievich, and K. A. Chao, Phys. Rev. Lett. **83**, 4884 (1999).
[27] K. Blum, *Density Matrix Theory and Applications* (Plenum Press, New York, 1996).
[28] P. Borri, W. Langbein, J. Mørk, J. M. Hvam, F. Heinrichsdorff, M.-H. Mao, and D. Bimberg, Phys. Rev. B **60**, 7784 (1999).
[29] A. Uskov, A. Jauho, B. Tromborg, J. Mork, and R. Lang, Phys. Rev. Lett. **85**, 1516 (2000).
[30] P. Borri, W. Langbein, S. Schneider, U. Woggon, R. Sellin, D. Ouyang, and D. Bimberg, Phys. Rev. Lett. **87** (2001).